



## Aerodynamics Characteristics for Symmetric and Cambered Airfoils Using Conformal Mappings

<sup>1</sup>Garba, Mohammed, <sup>2</sup>N. H. Manjak, <sup>3</sup>S. Hamma and <sup>4</sup>M. S. Adamu

<sup>1</sup>Department of Science Education, Bauchi State University Gadau, Nigeria.

<sup>2, 3, 4</sup>Department of Mathematical Science, Abubakar Tafawa Balewa University Bauchi, Nigeria.

### ABSTRACT

One of the most important potential flow results obtained using conformal mapping are the solutions of the potential flows past a family of airfoil shapes. Solving problem of fluid flow around an airfoil is a highly complex task. However, reducing the problem to two-dimensional ideal fluid flow allows one to employ techniques of complex variables, in particular utilizing the geometrics properties of conformal mappings. In this study, we analysed two dimensional ideal fluid flow around a circular cylinder obtained by the superposition of simple elementary flows, then transform the solution (complex potential) to symmetric NACA 0012 and cambered NACA4412 airfoil by means of conformal transformations, and it was found that the lift and drag forces around a circular cylinder in the  $z$  plane remained unchanged around transformed airfoils in the  $w$  plane. MATLAB scripts were used to visualize the streamlines around the circular cylinder and the corresponding airfoils. The aerodynamic characteristics of lift and drag were computed at different angles of attack and the results was validated using XFOIL data. Comparatively the Karman-Trefftz airfoil outperformed Joukowsky airfoils in respect of efficiency and performance of the airfoils.

### 1. Introduction

In fluid dynamics, an area of significant practical importance is the study of airfoils. Understanding the design of applicable systems such as airplanes wings, and wind turbines requires a quantitative method of analyzing fluid flow and lift. Understanding lift at a higher level thus involves the physical modelling of the fluid flowing over an airfoil. While this physical modelling is obviously an area of interest to engineers', it is also a relevant field for students studying advanced Complex analysis.

Prior to the development of the computer, obtaining an accurate solution for the flow around an airfoil shape was a challenging task. The development of conformal transformations was therefore of great benefit, as it provides an analytic solution for the exact flow solution to select number of airfoil shapes. Christoper (2008).

Conformal mapping, which makes the computation of fluid flow around airfoil possible defined by

$$w = f(z) \quad (1)$$

is a complex function technique in which complicated geometries can be transformed by an appropriate mapping function to simpler ones which still preserves both the angles and orientation of the original geometry. Using this technique, the flow around an airfoil can be analysed as the flow around a circular cylinder for which an analytic form of solution is well known (Samuel 2018). Since the functions that describe the fluid flow satisfy the equation of Laplace, the conformal mapping method allows for lift calculations on the cylinder to be equated to those on the corresponding airfoil.

As is evident in the works of Simakov *et al* (2000), Bjom (2006) and Vassberg & Jameson (2010). For aerodynamic applications, the conformal mapping function commonly used is the Joukowsky transformation defined by

$$w = f(z) = z + \frac{\lambda^2}{z} \quad (2)$$

where  $w$  is the function in the transformed plane and  $\lambda$  is the parameter of the transformation that determines the resulting shape of the transformed function geometry (Maloneka & De Almeida, 2010). This is because equation (2) has the property of transforming circles in the  $z$  plane into shapes that resemble airfoils in the  $w$  plane (Benson & Thomas, 1996).

Nyandwi (2018) modelled two dimensional ideal fluid flow around airfoil using Joukowsky conformal transformation, however, pointed out two drawbacks of the Joukowsky airfoils. These drawbacks include a knife-edge cusp at the trailing edge which presents manufacturing and structural integrity difficulties and the fact that the profiles of the Joukowsky airfoil have the maximum thickness very close to the leading edge, which results in adverse pressure gradient over most of the upper surface leading to earlier boundary layer transition and higher skin friction drag. Therefore, suggested for using Karman-Trefftz transformation as an improved transformations to avoid the two drawbacks of the Joukowsky airfoils.

This work is therefore, suggests replacement of the Joukowski conformal map in the original method of Nyandwi (2018) with the Karman-Trefftz conformal map equation (3) which has a parameter that controls the trailing edge angle which may likely improve the accuracy of the original method of Nyandwi (2018) since the airfoil generated in this case will be more truly the images of the cylinder in construction a physical model used to represent the inviscid, incompressible fluid flow around an airplane wing (airfoil).

$$\frac{w+\lambda c}{w-\lambda c} = \left(\frac{z+\lambda}{z-\lambda}\right)^\lambda, \quad \left(\lambda = 2 - \frac{\tau}{\pi}\right) \quad (3)$$

We equally seek to compute aerodynamics characteristics of symmetric NACA0012 and cambered NACA 4412 airfoils in order to determine the efficiency and performance of airfoils obtained from the two methods as an extension of the work of Swem (2018).

The efficiency and performance of aircraft depend on the aerodynamic characteristics (lift, drag, lift to drag ratio) of the wing which is in form of airfoil shape. Mohammed Adel (2019). Lift and drag forces are generated based on the airfoil geometry and the operating conditions. The airfoil geometry are the shape of the airfoil, the airfoil span, and the twist angle. Some of the operating conditions are mach number, the ambient pressure, and angle of attack (AOA). Basically, an airplane wing generates lift by diverting the motion of fluid flowing over its surface in a downward direction, resulting in an upward reaction force by Newton's third law (Anderson, 2001). Lift force is the perpendicular force to the chord generated due to the pressure difference between the lower and upper surface of the airfoil. The other component of the force which is parallel to the chord is called drag force, as shown in figure 1.

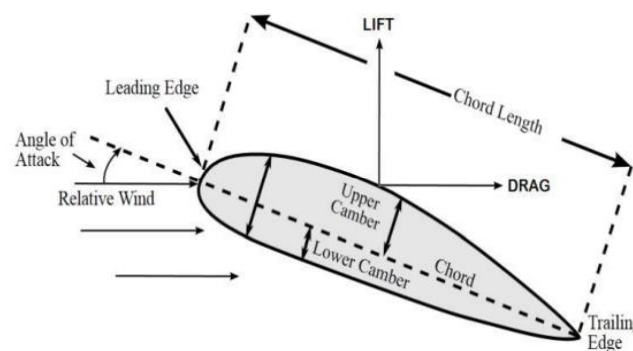


Figure 1: General Section of an airfoil (Stewart & William 2010)

This work focuses on modelling two-dimensional fluid flow around the airplane wing constructed by superposition of three elementary flows (uniform, doublet and vortex flows) around circular cylinder using Karman-Trefftz conformal mapping techniques. The flow around the air plane wings can be considered as an ideal fluid flow, that is fluid motions that are steady, inviscid, incompressible, and irrotational (Anderson, 2007). Considering the fluid flow around the airfoil as an inviscid and incompressible still allows for an accurate model provided certain conditions are met. One of these conditions is that the airplane wing must be moving through the fluid at subsonic speeds; this is very crucial because at speeds approaching the speed of sound, shock waves occur in which the fluid flow no longer becomes continuous, and the perfect fluid idealization breaks down. In particular, we will build our models for airfoils moving through flows regions where the compressibility effects in the flow can be negligible (Mach number between 0.0 and 0.4). Another assumption is that the flow around the airplane wing satisfies the Kutta Condition (figure 2).



Figure 2: Inviscid flow over an airfoil with the Kutta condition satisfied. The flow meets smoothly at the trailing edge. (Milne-Thomson, 1958).

The Kutta condition is that the fluid flowing over the upper and lower surfaces of the airfoil meets smoothly at the trailing edge of the airfoil and explains how an inviscid fluid can generate lift. Thus, the Kutta condition accounts for the friction at the boundary of an airfoil that is essential for lift to be generated under other additional constraints on the flow around an airfoil (Anderson 2001). With reference to the law of conservation of mass, a fluid flow is said to be an incompressible flow if its density  $\rho$  is constant, in contrast, it is called compressible when  $\rho$  varies. The fluid flow where the density is precisely constant does not exist in nature, but, there are many aerodynamic problems which can be modelled as incompressible flows without loss of accuracy (Anderson, 2007).

In this case the equation of continuity

$$\frac{\partial \rho}{\partial t} + \frac{\partial(\rho u)}{\partial x} + \frac{\partial(\rho v)}{\partial y} + \frac{\partial(\rho w)}{\partial z} = 0 \quad (4)$$

reduces to

$$\frac{\partial^2 \phi}{\partial x^2} + \frac{\partial^2 \phi}{\partial y^2} = 0 \quad (5)$$

In the same way, it can be shown that

$$\frac{\partial^2 \psi}{\partial x^2} + \frac{\partial^2 \psi}{\partial y^2} = 0. \quad (6)$$

Furthermore, the absence of frictional shear forces acting on elements of an inviscid fluid causes the motion of the fluid to be purely translational, allowing the flow over an airfoil to be modelled as irrotational. Again this irrotationality property of the fluid motion results in equation (7)

$$\nabla \times \vec{V} = 0 \quad (7)$$

due to the fact that the curl of the velocity vanishes. Since the motion is irrotational, its velocity field  $V$  can be expressed as the gradient of a scalar function  $\phi$  in the sense that  $V = \nabla\phi$ . We call  $\phi$  the velocity potential, and the flows that result from a velocity potential are known as potential flows. We saw in (6) that  $\phi$  satisfies the Laplace equation

$$\nabla^2 \phi = 0. \quad (8)$$

and solutions to this equation are referred to as harmonic functions. Since Laplace's equation is a linear homogeneous second order partial differential equation, the sum of particular solutions to the differential equation is also a solution (Anderson, 2007). This means that we can study complicated stream functions that one built up from simpler ones.

Due to the fact that the air plane wings have complicated geometries; it is difficult to directly solve for the fluid flow around them using Laplace equation and potential flow theory. To do this in a more efficient way; we define a complex potential function in the  $z$ -plane as

$$\Theta(z) = \phi(x, y) + i\psi(x, y), \quad (9)$$

called the complex velocity potential, using the velocity potential  $\phi(x, y)$  and the stream function  $\psi(x, y)$ . It is an analytic function. Since  $\phi$  and  $\psi$  are continuous functions of their argument  $z = x + iy$ , so is  $\Theta$ .

$$\frac{\partial \phi}{\partial x} = \frac{\partial \psi}{\partial y}, \quad \frac{\partial \psi}{\partial x} = -\frac{\partial \phi}{\partial y} \quad (10)$$

That means that  $\Theta$  satisfies the Cauchy-Riemann equations.

Note that  $\phi, \psi$  satisfy Laplace's equation. This is always true of the real or imaginary part of an analytic function, and such functions are called harmonic.

## Methodology

From the fact that, when the complex potential function is transformed using conformal mapping techniques, the potential and stream functions remained unchanged. In this work we first solve the flow around a cylinder in the  $z$  plane, and then transform this solution to an airfoil in the  $w$  plane using Karman-Trefftz conformal transformation. We also computed the aerodynamic characteristics around the Karman-Trefftz airfoils using MATLAB scripts.

Conformal transformation requires that the velocity potential and stream function of the cylinder be expressed as a complex function, just as the airfoil shape must also be defined using complex variables, given by

$$w(z) = \phi + i\psi \quad (11)$$

If, moreover,  $\psi(x, y)$  denotes a harmonic conjugate of  $\phi(x, y)$ , the velocity vector is tangent to the curve  $\psi(x, y) = c$ . That is in the same direction with curve (Bear 1972)

The curve

$$\psi(x, y) = c \quad (12)$$

is called the streamline of the flow, and the function  $\psi$  is the stream function. In particular, a boundary across which fluid can not flow is a streamline (Brown & Churchill, 2009).

To compute the complex potential, this method assumes a solution for the complex potential of the flow past the cylinder given as

$$w(z) = V_\infty \left( z + \frac{R^2}{z} \right) + i \frac{\Gamma}{2\pi} \ln(z) \quad (13)$$

which is obviously the superposition of the uniform, doublet and vortex flows.

Equation (12) decomposes into real and imaginary components

$$w(z) = V_\infty \left( r + \frac{R^2}{r} \right) \cos \theta - \frac{\Gamma}{2\pi} \theta + i \left[ V_\infty \left( r - \frac{R^2}{r} \right) \sin \theta + \frac{\Gamma}{2\pi} \ln(r) \right] \quad (14)$$

which yields, the stream function  $\psi$  of the combined flow as

$$\psi = V_{\infty} r \sin \theta \left(1 - \frac{R^2}{r^2}\right) + \frac{\Gamma}{2\pi} \ln r \quad (15)$$

### Karman-Trefftz Mapping from Circular Cylinder to Airfoil

In this approach, the Karman-Trefftz conformal transformation defined as

$$\frac{w+\lambda c}{w-\lambda c} = \left(\frac{z+\lambda}{z-\lambda}\right)^{\lambda}$$

Let  $\tau$  be the angle between the tangents of the upper and lower airfoil surfaces at the trailing edge, then is related to  $\lambda$  as

$$\tau = 2\pi - \lambda\pi \quad (16)$$

Such that,

$$\lambda = 2 - \frac{\tau}{\pi} \quad (17)$$

The constant  $c$  in equation (3) is estimated as  $1/2\lambda$  of the distance between the trailing edge and a point mid way between the leading edge and the centre of curvature of the nose.

In order to map the circular cylinder in  $z$ -plane into the airfoil in  $w$ -plane, the Karman-Trefftz method requires that the circular cylinder center be defined by  $x_c, y_c$ . and the trailing edge angle,  $\tau$ , is defined in degrees. Finally,  $c$ , which is the  $x$ -intercept, is set equal to unity. Lastly, the circulation is set in order to meet the Kutta condition to ensure smooth flow leaving the trailing edge.

The Kutta condition requires that the trailing edge  $T$  is a stagnation point where the fluid velocity vanishes identically (Anderson, 1991).

### Determination of the aerodynamic coefficient of the lift and drag for the NACA 0012 and NACA 4412 airfoils using conformal mapping method.

An airfoil's aerodynamic performance can be characterized by several factors such as the lift, drag etc. All are functions of the pressure and shear stress distribution across the surface of an airfoil. When improving an airfoil's performance, it is generally desired to increase the lift while maintaining or decreasing the drag. To uniformly evaluate the lift and drag forces a variety of airfoils and flows, the forces are non dimensionalized into the corresponding coefficient.

The generalized method for computation of the lift and drag forces on arbitrary airfoils can not be executed manually. Consequently, the method is coded in MATLAB for both symmetrical and cambered airfoils of the NACA four digit series family (see appendices I and II for the codes), respectively.

The lift coefficient is computed using the formula given as (Anderson 1991 and Karamcheti, 1966)

$$c_l = \frac{L_F}{\frac{1}{2}\rho_{\infty}V_{\infty}^2 A} \quad (18)$$

and drag coefficient defined as

$$c_d = \frac{D_F}{\frac{1}{2}\rho_{\infty}V_{\infty}^2 A} \quad (19)$$

where  $A$  is the area of a given airfoil which is  $1.6944m^2$  and  $1.9944m^2$  for symmetric 0012 and 4412 for Karman-Trefftz airfoils respectively.

For Karman-Trefftz 0012 Airfoil at  $\alpha = 1$ , Lift force is 2456.5 N/M, Drag force 174.67

$$c_l = \frac{2456.5}{0.5 \times 1.225 \times 10000 \times 1.6944} = 0.2367$$

$$c_d = \frac{174.67}{0.5 \times 1.225 \times 10000 \times 1.6944} = 0.01683$$

For Karman-Trefftz 4412 Airfoil at  $\alpha = 0$ , Lift force is 5168N/M, Drag force is 73.17N/M

$$c_l = \frac{5168}{0.5 \times 1.225 \times 10000 \times 1.9944} = 0.4231$$

$$c_d = \frac{73.17}{0.5 \times 1.225 \times 10000 \times 1.9944} = 0.00599$$

## Results

Conformal Mappings (Joukowski and Karman-Trefftz transformations) were exploited to simulate the flow around symmetric NACA 0012 and cambered NACA 4412 airfoils at various angles of attack ranging from  $0^\circ$  to  $10^\circ$ . The lift coefficient ( $c_l$ ) and drag coefficient ( $c_d$ ) computed using (18) and (19) from lift and drag forces generated by MatLab scripts. The lift to drag coefficients ratio ( $c_l/c_d$ ) were computed for determine aerodynamic efficiency and performance of the airfoils.

### Generating the Streamlines around Joukowski and Karman-Trefftz Airfoils

When a conformal transformation is applied to an offset circular cylinder, computational graphing program can be used to visualize the flow and establish lift and drag forces for several airfoils.

The contour plot of the imaginary component of the complex potential equation (12) gives the flow around the airfoil. The lift force is calculated using

$$L' = V_{\infty} \rho_{\infty} \Gamma$$

where  $\Gamma$  for symmetric airfoil is given by;

$$\Gamma = \frac{2rV_{\infty} \sin \alpha}{2\pi} \tag{18}$$

and for cambered airfoil is given by

$$\Gamma = 4r\pi v_{\infty} \sin(\alpha + \beta) \tag{19}$$

The streamlines is visualised using MatLab code.

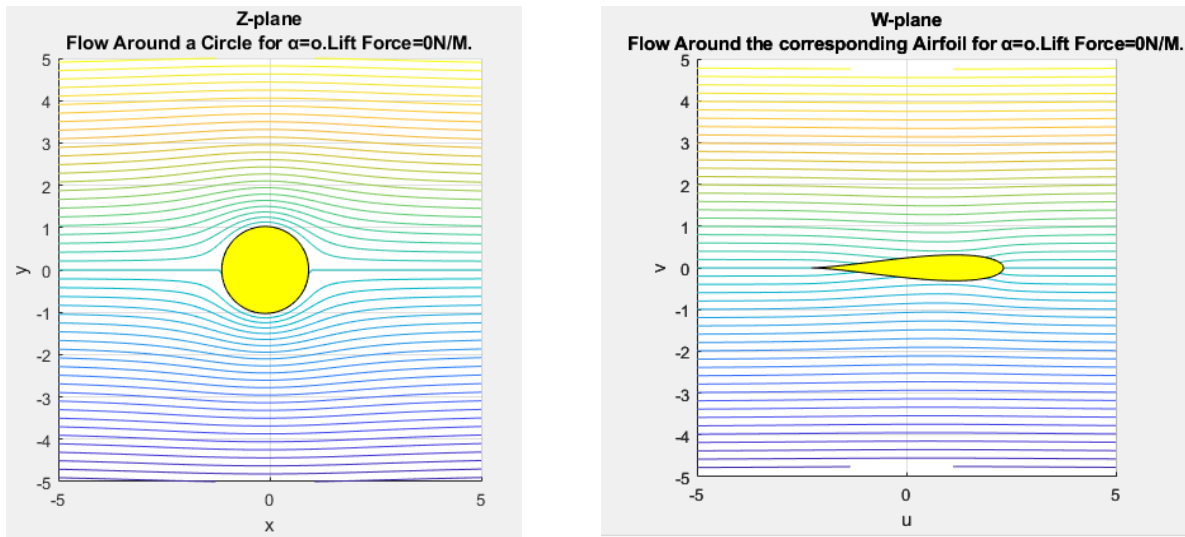


**Figure 3:** The streamlines around circular cylinder plot computed in the z plane and the corresponding symmetric Joukowski airfoil. The plot was generated with  $V_{\infty} = 100\text{m/s}$ ,  $\alpha = 5^\circ$ , and  $\rho = 1.225 \text{ kg/m}^3$ . The cylinder parameters used:  $x = -0.107\text{m}$ ,  $y = 0\text{m}$ ,  $r = 1.027\text{m}$ .

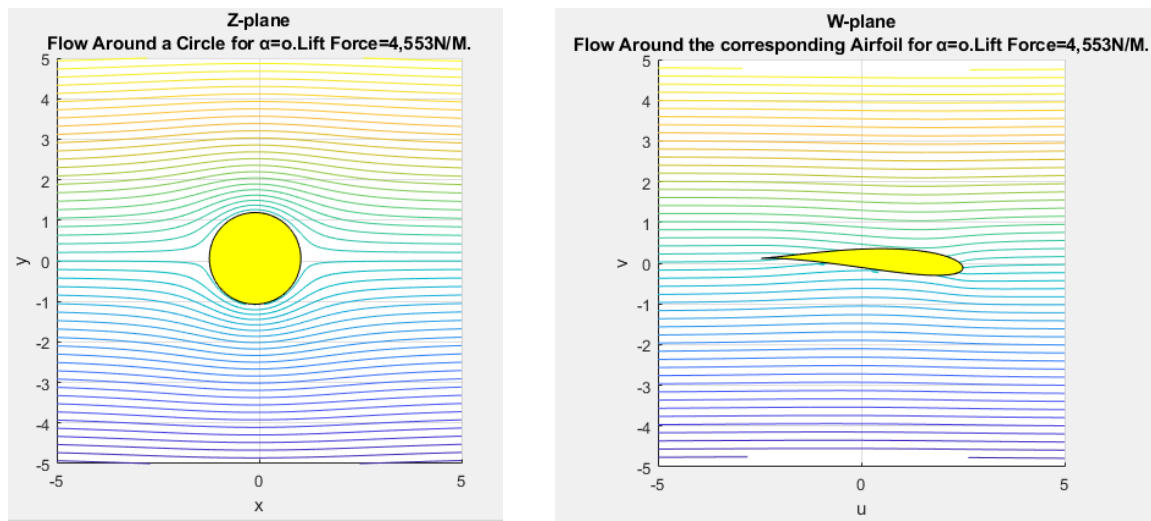


**Figure 4:** The streamlines around circular cylinder plot computed in the z plane and the corresponding cambered Joukowski airfoil. The plot was generated with  $V_{\infty} = 100\text{m/s}$ ,  $\alpha = 5^\circ$ , and  $\rho = 1.225 \text{ kg/m}^3$ . The cylinder parameters used:  $x = -0.100\text{m}$ ,  $y = 0.6\text{m}$

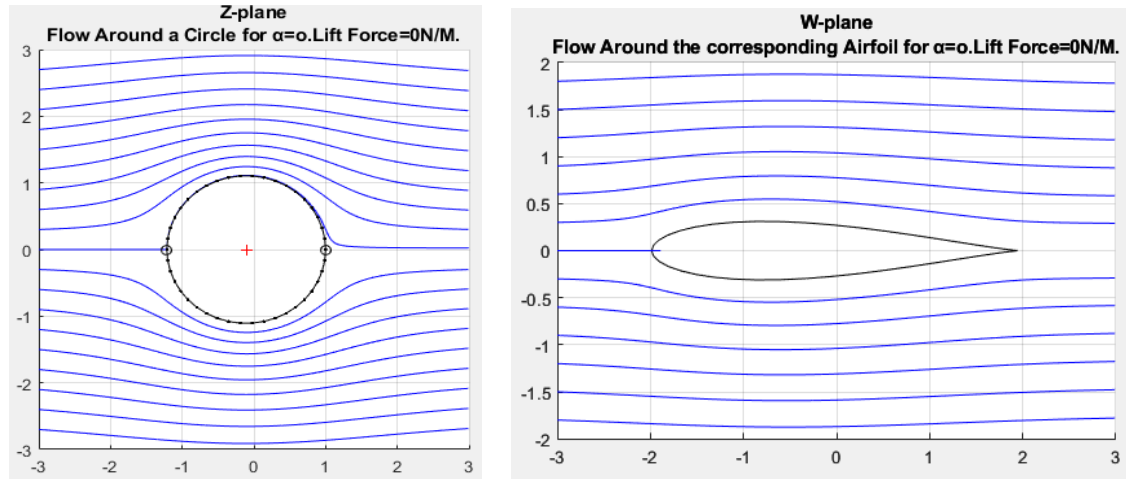


Figure 5: The streamlines around circular cylinder plot computed in the z plane and the corresponding symmetric Karman-Trefftz airfoil. The plot was generated with  $V_\infty = 100\text{m/s}$ ,  $\alpha = 5^\circ$ , and  $\rho = 1.225\text{ kg/m}^3$ . The cylinder parameters used:  $x_c = -0.107\text{m}$ ,  $y_c = 0.0\text{m}$ .

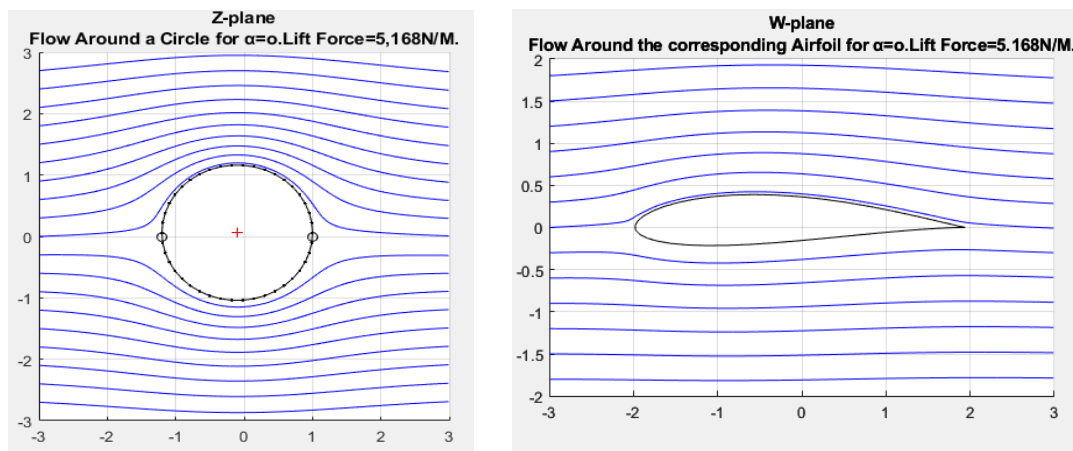


Figure 6: The streamlines around circular cylinder plot computed in the z plane and the corresponding cambered Karman-Trefftz airfoil. The plot was generated with  $V_\infty = 100\text{m/s}$ ,  $\alpha = 5^\circ$ , and  $\rho = 1.225\text{ kg/m}^3$ . The cylinder parameters used:  $x_c = -0.100\text{m}$ ,  $y_c = 0.6\text{m}$ .

Plots of the coefficients of lift and drag curves for NACA 0012 airfoils using Joukowski method, Karman-Trefftz method and XFOIL data.

Table 1: Coefficients of Lift and Drag Data as a Function of Angle of Attack for Symmetric Karman-Trefftz 0012 Airfoil

AOA( $\alpha$ )	LIFT COEFFICIENT(CL)	DRAG COEFFICIENT(CD)	CL/CD COEFFICIENTS
0	0.000	0.01683	0.00
1	0.2367	0.01494	15.84
2	0.3243	0.01296	25.02
3	0.3987	0.01287	30.96
4	0.4732	0.01366	34.63
5	0.5674	0.01581	35.87
6	0.6237	0.01804	34.56
7	0.6984	0.02217	31.67
8	0.7863	0.02723	28.87
9	0.8774	0.03435	25.54
10	0.9013	0.04582	20.63

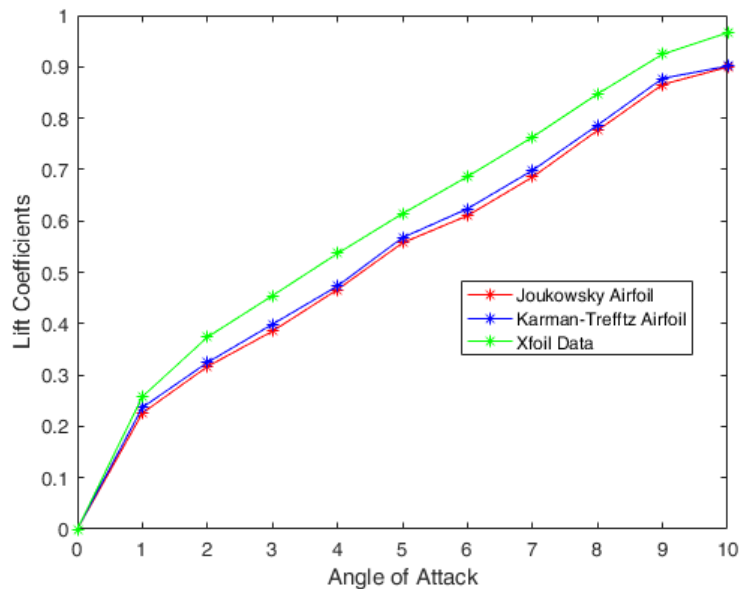
Table 2: Coefficients of Lift and Drag Data as a Function of Angle of Attack for Symmetric Joukowski 0012 Airfoils

AOA( $\alpha$ )	LIFT COEFFICIENT(CL)	DRAG COEFFICIENT(CD)	CL/CD COEFFICIENTS
0	0.000	0.01682	0.00
1	0.2258	0.01455	15.51
2	0.3164	0.01271	24.87
3	0.3852	0.01281	30.07
4	0.4663	0.01366	34.12
5	0.5572	0.01581	35.23
6	0.6102	0.01794	34.00
7	0.6853	0.02201	31.13
8	0.7762	0.02738	28.33
9	0.8654	0.03461	25.00
10	0.8994	0.04472	20.11

Table 3: Coefficients of Lift and Drag Data as a Function of Angle of Attack for NACA 0012 Airfoils obtained by Xfoil

AOA( $\alpha$ )	LIFT COEFFICIENT(CL)	DRAG COEFFICIENT(CD)	CL/CD COEFFICIENTS
0	0.0000	0.01693	0.000
1	0.2578	0.01574	16.378
2	0.3737	0.01444	25.879
3	0.4544	0.01440	31.555
4	0.5365	0.01520	35.296
5	0.6141	0.01674	36.684
6	0.6862	0.01958	35.045
7	0.7631	0.02348	32.50
8	0.8471	0.02869	29.525
9	0.9246	0.03526	26.222
10	0.9661	0.04582	21.08

<http://airfoiltools.com/polar/details?polar=xf-n0012-il>

Figure 7: Comparison of the Lift coefficient ( $c_l$ ) Curves for NACA 0012 Airfoil between Joukowski, Karman Trefftz Airfoils and Xfoil data.

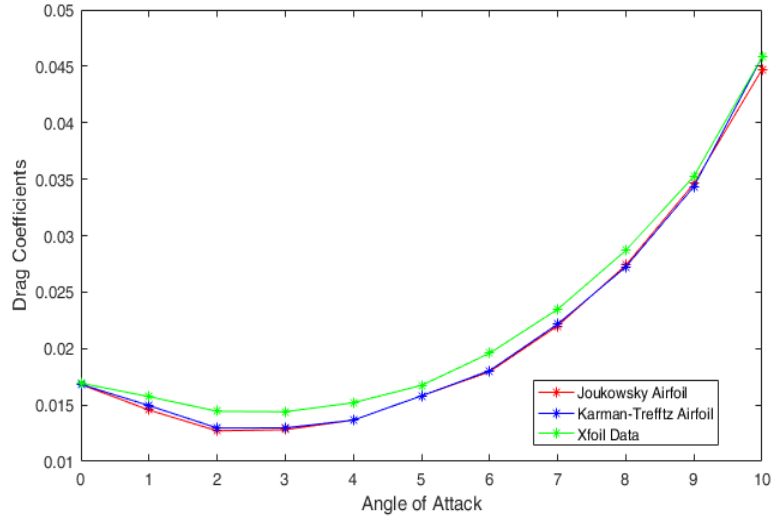


Figure 8: Comparison of the Drag coefficient ( $c_d$ ) Curves for NACA 0012 Airfoil between Joukowsky, Karman Trefftz Airfoils and Xfoil data.

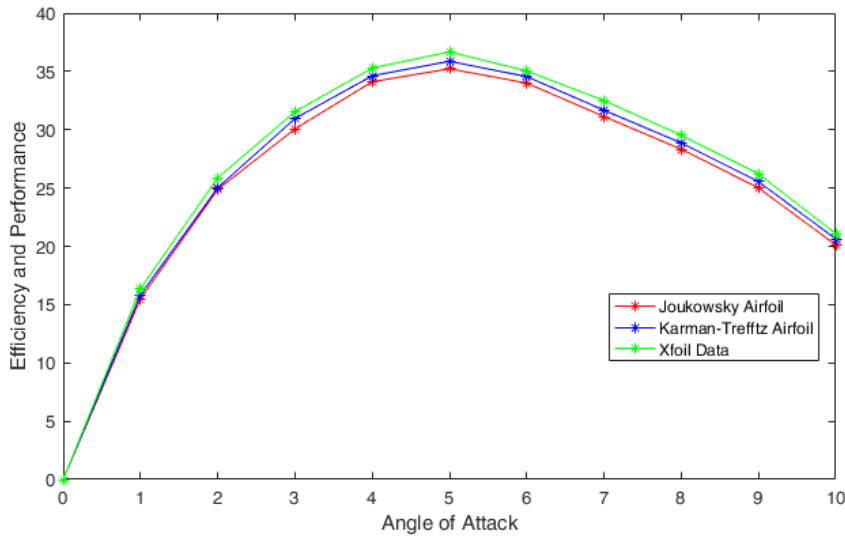


Figure 9: Comparison of the Coefficients of Lift to Drag ratio ( $c_l/c_d$ ) Curves for NACA 0012 Airfoil between Joukowsky, Karman Trefftz Airfoils and Xfoil data.

Plots of the coefficients of lift and drag curves for NACA 4412 airfoils using Joukowsky method, Karman-Trefftz method and XFOIL data.

Table 4: Coefficients of Lift and Drag Data as a Function of Angle of Attack for Cambered Karman-Trefftz 4412 Airfoil

AOA( $\alpha$ )	LIFT COEFFICIENT(CL)	DRAG COEFFICIENT(CD)	CL/CD COEFFICIENTS
0	0.4231	0.00599	70.56
1	0.5087	0.00523	97.11
2	0.6334	0.00562	112.61
3	0.7021	0.00573	122.33
4	0.8563	0.00675	126.78
5	0.9386	0.00731	127.54
6	0.9786	0.00771	126.89
7	1.0536	0.00900	116.97
8	1.1641	0.01166	99.76



9	1.254	0.01425	88.00
10	1.2981	0.01617	80.23

Table 5: Coefficientns of Lift and Drag Data as a Function of Angle of Attack for Cambered Joukowsky 4412 Airfoil

AOA( $\alpha$ )	LIFT COEFFICIENT(CL)	DRAG COEFFICIENT(CD)	CL/CD COEFFICIENTS
0	0.4222	0.00599	70.48
1	0.5005	0.00515	97.00
2	0.6122	0.00546	111.97
3	0.6947	0.00570	121.78
4	0.7876	0.00624	126.32
5	0.8582	0.00679	126.32
6	0.9001	0.00714	126.00
7	0.9564	0.00826	115.76
8	1.0241	0.01035	98.89
9	1.1983	0.01368	87.57
10	1.2064	0.01513	79.72

Table 6: Coefficientns of Lift and Drag Data as a Function of Angle of Attack for NACA 0012 Airfoils obtained by Xfoil

AOA( $\alpha$ )	LIFT COEFFICIENT(CL)	DRAG COEFFICIENT(CD)	CL/CD COEFFICIENTS
0	0.0000	0.01693	0.000
1	0.2578	0.01574	16.378
2	0.3737	0.01444	25.879
3	0.4544	0.01440	31.555
4	0.5365	0.01520	35.296
5	0.6141	0.01674	36.684
6	0.6862	0.01958	35.045
7	0.7631	0.02348	32.50
8	0.8471	0.02869	29.525
9	0.9246	0.03526	26.222
10	0.9661	0.04582	21.08

<http://airfoiltools.com/polar/details?polar=xf-n0012-il>

Table 7: Coefficientns of Lift and Drag Data as a Function of Angle of Attack for NACA 4412 Airfoils obtained by Xfoil

AOA( $\alpha$ )	LIFT COEFFICIENT(CL)	DRAG COEFFICIENT(CD)	CL/CD COEFFICIENTS
0	0.4833	0.00678	71.283
1	0.5842	0.00594	98.350
2	0.7055	0.0622	113.42
3	0.8405	0.00681	123.42
4	0.9210	0.00722	127.562
5	1.0254	0.00797	128.657
6	1.1280	0.00884	127.601
7	1.2208	0.01036	117.837
8	1.2973	0.01288	100.722
9	1.3676	0.01527	89.561

<b>10</b>	<b>1.4317</b>	<b>0.01746</b>	<b>81.9988</b>
-----------	---------------	----------------	----------------

<http://airfoiltools.com/polar/details?polar=xf-n4412-il>

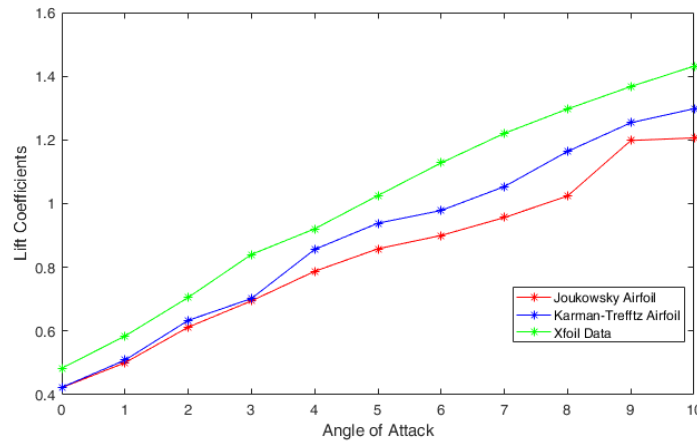


Figure 10: Comparison of the Lift coefficient ( $c_l$ ) Curves for NACA 4412 Airfoil between Joukowsky, Karman Trefftz Airfoils and XFOIL data.

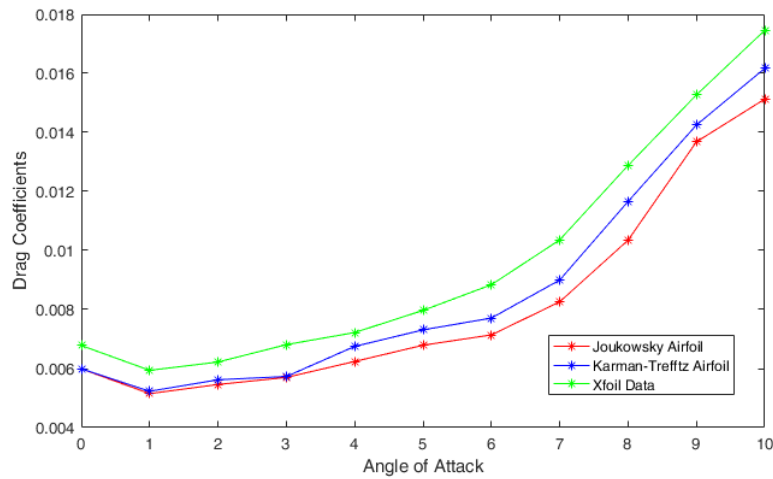


Figure 11: Comparison of the Drag coefficient ( $c_d$ ) Curves for NACA 0012 Airfoil Between Joukowsky, Karman Trefftz Airfoils and XFOIL data.

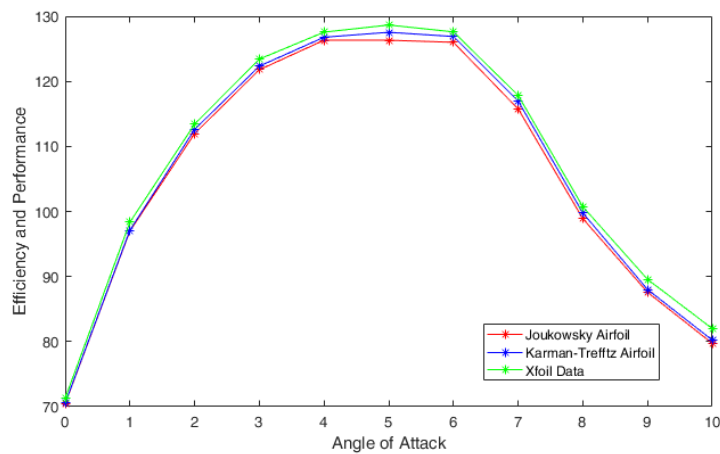


Figure 12: Comparison of the Coefficients of Lift to Drag ratio ( $c_l/c_d$ ) Curves for NACA 4412 Airfoil between Joukowsky, Karman Trefftz Airfoils and XFOIL data.

---

## Result Discussion

When a conformal transformation is applied to an offset circular cylinder, one can get airfoils by the use of instance of Matlab program. The streamlines generated by the imaginary component of the complex potential (12) is the flow solution around cylinder and corresponding airfoil. As is evident from Joukowski airfoils (figure 1 and 2), Joukowski map fixes the trailing edge angle permanently at  $0^\circ$  resulted in cusp trailing edge while Karman-Trefftz airfoils (3 and 4) show blunt trailing edge, therefore the drawback experience by Nyandwi (2018) has been resolved. Also figure 8 and 11 indicate that the Karman-Trefftz airfoils outperformed Joukowski airfoils in respect of efficiency and performance ( $c_l/c_d$ )

---

## Conclusion

The main goal of our paper was to apply the conformal mapping technique to model the two dimensional fluid flow around an airplane wing. We reviewed the mathematical model used to describe the two dimensional ideal fluid flow around a circular cylinder obtained by the superposition of simple elementary flows. This model was implemented in MATLAB in order to visualize the streamlines and the equipotential curves for each elementary flow needed in the process of modeling the flow around a circular cylinder.

In this research paper the conformal mapping aspect of the method of Nyadwi (2018) is modified by replacing the Joukowski map in the method by the Karman-Trefftz map to also account for the nonzero angles at the trailing edge of real airfoils. The modified method has given reasonable predictions on the efficiency and performance for the NACA 0012 and 4412 airfoils and has outperformed the original version of the method by Nyandwi (2018).

---

## References

- Anderson, J. D., 2001, Fundamentals of Aerodynamics, McGraw-Hill
- Anderson, J.D. 2007 Fundamentals of Aerodynamics, 4th Edition, New York: Mc GrawHill.
- Anderson, J.D, (1991), Fundamentals of Aerodynamics, MCGraw-Hill, New York, Pp. 93 – 275.
- Bear J., (1972). Dynamics of Fluids in Porous Media. Canada: American Elsevier,.
- Benson S. & Thomas J., (1996). Interactive Educational Tool for Classical Airfoil Theory. Cleveland, Ohio: NASA Lewis Research Center, Oct.
- <http://www.grc.nasa.gov/WWW/K-12/airplane/FoilTheory.pdf>
- Bjom, R. (2006). Conformal Mapping Potential Flow around a Wing Section Used as a Test Case for the Inviscid Part of Rans Solver. Paper presented at the European Conference on Computational Fluid Dynamics, TU Delt, The Netherlands.
- Brown J. W. & Churchill R.V. (2009). Complex Variables and Application, McGraw-Hill Carlos Alberto Abello Muñoz, 2018. A Survey of Joukowski Airfoil and von Karman Vortex Street, *Contemporary Engineering Sciences*, 11(99), 4921 - 4928
- HIKARI Ltd, www.m-hikari.com <https://doi.org/10.12988/ces.2018.810540>
- Christopher J. Peterson (2008), Minimum Pressure Envelope Cavitation Analysis Using Two- Dimensional Panel Method, Msc Dissertation in Mechanical Engineering, Massachusetts Institute of Technology.
- Milne-Thomson L.M, 1985. C.B.E., Theoretical Aerodynamics, Fourth Edition, Dover Publications, INC. New York.
- Mohammed Adel (2019), A Comparative Study for Different Shapes of Airfoils, *International Journal of Mechanical Engineering* <http://www.iasar.org/iasar/journals/ijme>
- Maloneka H.R. & De Almeida R., (2010), A note on a generalized Joukowski transformation, *Applied Mathematics Letters* : 23 :1174–1178 : [www.elsevier.com/locate/aml](http://www.elsevier.com/locate/aml)
- Nyandwi Bosco (2018), Application of conformal Mapping to the Fluid flow, Msc Dissertation, Department of Mathematics, University of Rwanda.
- Samuel . S . T., (2017). Computation of Pressure Distribution and Aerodynamic Lift On Arbitrary Airfoils Using Conformal Mappings. Ph.D .Dissertation, Department of Mathematical Sciences, Abubakar Tafawa Balewa University Simakov, S.T., Dostovalova, A.S., and Tuck, E.O. (2000). A GUI for Computing Flows Past General Airfoils. Paper Presented at the Australasian MATLAB User Conference, Melbourne.
- Stewart A.L. and William J., 2010. Devenport “Panel methods for airfoils in turbulent flow” (*Journal of Sound and Vibration*) 329 (2010) 3709–3720
- Swem S. T and Otene E., (2020). *On the use of the Schwarz- Christoffel Transformation in the Solution and Analysis of Harmonic Dirichlet Problems of the Ideal Fluid Flows. Global Scientific Journals*, vol.8, Issue 3, ISSN 2320-9186.
- Vassberg, J. C. And Jameson, A. (2010). In pursuit of Grid Convergence for Two-Dimensional Euler Equations. *Journal of Aircraft*. **14**: 1152-1166

<http://airfoiltools.com/polar/details?polar=xf-n0012-i> retrieve on 02/07/23

<http://airfoiltools.com/polar/details?polar=xf-n4412-i> retrieve on 02/07/23